Available online at www.sciencedirect.com
ScienceDirect
Geochimica et Cosmochimica Acta 70 (2006) 5676–5691
Geochimica
www.elsevier.com/locate/gca

BRYOCARB: A process-based model of thallose liverwort carbon isotope fractionation in response to CO_2, O_2, light and temperature

Benjamin J. Fletcher, Stuart J. Brentnall, W. Paul Quick, David J. Beerling *

Department of Animal and Plant Sciences, University of Sheffield, Sheffield, S10 2TN, UK

Received 1 August 2005; accepted in revised form 30 January 2006

Abstract

Evidence from laboratory experiments indicates that fractionation against the heavy stable isotope of carbon ($\Delta^{13}C$) by bryophytes (liverworts and mosses) is strongly dependent on atmospheric CO_2. This physiological response may therefore provide the basis for developing a new terrestrial CO_2 proxy [Fletcher, B.J., Beerling, D.J., Brentnall, S.J., Royer, D.L., 2005. Fossil bryophytes as recorders of ancient CO_2 levels: experimental evidence and a Cretaceous case study. *Global Biogeochem. Cycles* **19**, GB3012]. Here, we establish a theoretical basis for the proxy by developing an extended model of bryophyte carbon isotope fractionation (BRYOCARB) that integrates the biochemical theory of photosynthetic CO_2 assimilation with controls on CO_2 supply by diffusion from the atmosphere. The BRYOCARB model is evaluated against measurements of the response of liverwort photosynthesis and $\Delta^{13}C$ to variations in atmospheric O_2, temperature and irradiance at different CO_2 concentrations. We show that the bryophyte proxy is at least as sensitive to variations in atmosphere CO_2 as the two other leading carbon isotope-based approaches to estimating palaeo-CO_2 levels ($\delta^{13}C$ of phytoplankton and of paleosols). Mathematical inversion of BRYOCARB provides a mechanistic means of estimating atmospheric CO_2 levels from fossil bryophyte carbon that can explicitly account for the effects of past differences in O_2 and climate.

1. Introduction

The major end-products of mathematical models of the long-term carbon cycle, such as those pioneered by Berner (e.g., Berner, 1991, 1994; Berner and Kothavala, 2001), are Phanerozoic histories of a primary greenhouse gas, atmospheric CO_2 (Tajika, 1998; Wallmann, 2001; Kashiwagi and Shikazono, 2003; Berner, 2004; Bergman et al., 2004). These histories allow serious investigation of the link between CO_2 and climate change on geologic timescales. Critically, this endeavour also requires independent means of gauging levels of the gas in the ancient atmosphere. The four main pre-Quaternary proxies for this purpose are: the stable carbon isotope composition ($\delta^{13}C$, ‰) of pedogenic minerals (Cerling, 1991; Yapp and Poths, 1992), the $\delta^{13}C$ of phytoplankton (Freeman and Hayes, 1992; Pagani et al., 1999; Laws et al., 2002), the vascular plant stomatal index (Van der Burgh et al., 1993; McElwain and Chaloner, 1995; Royer et al., 2001b; Beerling and Royer, 2002), and the $\delta^{11}B$ of fossilized calcium carbonate shells of planktonic foraminifera (Pearson and Palmer, 2000). Significant uncertainties are associated with estimates of past CO_2 concentrations using each of these (Royer et al., 2001a), indicating the continuing need to search for alternative methods of assaying the chemical composition of the ancient atmosphere.

Recent laboratory experiments have offered the basis for a new terrestrial CO_2 proxy by showing isotopic discrimination against the rarer of the two stable isotopes of carbon (termed $\Delta^{13}C$, in ‰) in bryophytes (liverworts and mosses) is strongly dependent upon the growth CO_2 concentration (Fletcher et al., 2005) (Fig. 1). Plant $\Delta^{13}C$ is predominantly a function of the ratio of internal to external

* Corresponding author. Fax: +44 114 222 0002.
E-mail address: d.j.beerling@sheffield.ac.uk (D.J. Beerling).

0016-7037/$ - see front matter © 2006 Elsevier Inc. All rights reserved.
doi:10.1016/j.gca.2006.01.031

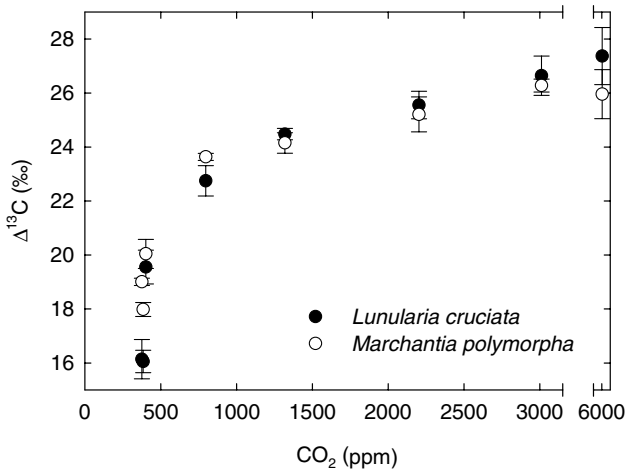

Fig. 1. The response of stable carbon isotope discrimination ($\Delta^{13}C$) in two liverwort species grown at different concentrations of atmospheric CO_2 in controlled environments. Values are means ± standard error. Data from Fletcher et al. (2005).

CO_2 concentration (C_i/C_a), averaged over the lifetime of the tissue (Farquhar et al., 1989). $\Delta^{13}C$ is therefore controlled by C_a (ppm), the kinetics of Rubisco (the primary carboxylating enzyme, ribulose-1,5-bisphosphate carboxylase/oxygenase), and the resistance to diffusion of CO_2 into the photosynthetic tissues. The strong dependency of bryophyte $\Delta^{13}C$ on CO_2 occurs because, unlike vascular plants, bryophytes lack stomata to regulate their resistance to inward CO_2 diffusion. As a result, the intercellular CO_2 concentration (C_i, ppm) is maintained at a concentration below C_a to an extent that is proportional to the rate of photosynthesis, a feature itself largely controlled by C_a (alongside other environmental factors). C_a can therefore be determined for a given $\Delta^{13}C$ if the responses of photosynthesis (A) and resistance (r) to CO_2 are known, assuming other environmental effects can be factored out (White et al., 1994; Figge and White, 1995). In effect, isotopic fractionation in astomatous liverworts and mosses can be regarded as the terrestrial equivalent of marine phytoplankton without carbon-concentrating mechanisms (CCMs) whose $\Delta^{13}C$ is primarily controlled by the rate of uptake of CO_2 dissolved in seawater (Laws et al., 1995; Popp et al., 1998).

We originally investigated the utility of the proxy by developing and calibrating a model describing the dependency of bryophyte isotopic fractionation on atmospheric CO_2 (Fletcher et al., 2005). In that isotopic model, we combined the responses of photosynthesis and resistance to CO_2 into a single 'lumped' term, $A \cdot r$, that varied empirically with CO_2 to influence C_i/C_a. However, a generalized mechanistic theory for the proxy is required to accurately assess how environmental factors interact with CO_2, and each other, to control the photosynthetic demand for CO_2, and the resistance to inward CO_2 diffusion.

Here, therefore, we describe an extended mechanistic model of carbon isotope fractionation in liverworts (BRYOCARB, BRYOphyte CARBon isotope model) designed to achieve this aim. BRYOCARB incorporates a well-validated mechanistic model of CO_2 assimilation in C_3 plants describing the demand for CO_2 (Farquahar et al., 1980; von Caemmerer and Farquhar, 1981) into the model of C_3 plant carbon isotope discrimination (Farquhar et al., 1982, 1989; White et al., 1994; Fletcher et al., 2005). The coupled isotope-photosynthesis model includes the response of r to CO_2 to describe the limitation on CO_2 supply to the photosynthetic tissue.

We evaluate the performance of BRYOCARB by simulating the photosynthetic and $\Delta^{13}C$ responses of liverworts to variations in O_2, irradiance and temperature at two atmospheric CO_2 concentrations. Simulations are evaluated against gas exchange and $\Delta^{13}C$ measurements of liverworts over a similar range of conditions. We next undertake a series of sensitivity analyses designed to (i) assess the likely impact of variations in O_2, irradiance and temperature on the CO_2 dependency of $\Delta^{13}C$ and (ii) model variations in liverwort $\Delta^{13}C$ over the Phanerozoic by driving BRYOCARB with predicted changes in O_2 (Berner, 2001), CO_2 (Berner and Kothavala, 2001), and greenhouse forcing of climate. Finally, we analyze the utility of fossil liverwort $\Delta^{13}C$ for reconstructing ancient CO_2 levels, by comparing its sensitivity to CO_2 with that of the CO_2 proxies based on the $\delta^{13}C$ of paleosol (Cerling, 1991; Yapp and Poths, 1992) and phytoplankton (Freeman and Hayes, 1992; Pagani et al., 1999; Laws et al., 2002) fossil carbon.

2. The BRYOCARB model

2.1. Background

The well-established model for the isotopic composition for plants with the C_3 photosynthetic pathway is defined as (Farquhar et al., 1982) (see Appendix A for notation and values not described in the text):

$$\delta^{13}C_p = \delta^{13}C_a - a - (b-a)\left(\frac{C_i}{C_a}\right) + \frac{\left(f\Gamma_* + \frac{er_d(C_i-\Gamma_*)}{A+r_d}\right)}{C_a}, \quad (1)$$

where a and b are the fractionations associated with diffusion and carboxylation by Rubisco, respectively. The last term on the right-hand side of Eq. (1) exerts a minor influence on the difference between $\delta^{13}C_p$ (plant stable carbon isotope composition, ‰) and $\delta^{13}C_a$ (air stable carbon isotope composition, ‰) which, with a and b taken as constants, means that C_i/C_a dominates. Bryophytes lack the stomata and thick cuticles of vascular plants and are unable to regulate CO_2 uptake and H_2O loss. As a result, C_i/C_a is controlled by simple diffusion (Proctor, 1982) and depends on (i) the atmospheric CO_2 concentration (C_a), and (ii) the difference between the external and ambient CO_2 concentrations ($C_a - C_i$). $C_a - C_i$ is a function of the rate of CO_2 consumption by photosynthesis

(A, μmol m^{-2} s^{-1}) and the total resistance to inward CO_2 diffusion (r, m^2 s mol^{-1}), as described by:

$$C_a - C_i = A \cdot r. \tag{2}$$

Re-arranging Eq. (2) for C_i and substituting into Eq. (1) gives:

$$\delta^{13}C_p = \delta^{13}C_a - a - (b-a)\left(1 - \frac{r \cdot A}{C_a}\right) + \frac{f \cdot \Gamma_* + e \cdot \frac{r_d}{\left(\frac{A+r_d}{C_a - r \cdot A - \Gamma_*}\right)}}{C_a}, \tag{3}$$

which provides a reasonably complete description of the main physical and biological factors influencing bryophyte $\delta^{13}C$. Eq. (3) has been calibrated against experimental observations of rA and inverted to predict C_a from any given pair of bryophyte $\delta^{13}C$ and $\delta^{13}C_a$ values (Fletcher et al., 2005). Discrimination ($\Delta^{13}C$) is then calculated from $\delta^{13}C_a$ and $\delta^{13}C_p$ as:

$$\Delta^{13}C = \frac{\delta^{13}C_a - \delta^{13}C_p}{1 + \delta^{13}C_p/1000}. \tag{4}$$

2.2. Modelling liverwort photosynthetic CO_2 demand

A generalized process-based model of bryophyte $\delta^{13}C$ with the capacity to account for the effect of other environmental parameters (irradiance, temperature and atmospheric O_2 and CO_2 concentrations) requires a mechanistic description of photosynthetic CO_2 uptake. We utilized a biochemical model of C_3 photosynthesis (Farquahar et al., 1980) in which net photosynthetic rate (A) is defined as the minimum of either two alternative rates A_c or A_j. When the rate of photosynthesis is primarily controlled by carboxylation by Rubisco, A_c, the rate is defined as:

$$A_c = \frac{\gamma V_m C_i}{C_i + k_c(1 + o_i/k_o)} - r_d, \tag{5}$$

where V_m is the maximum rate of carboxylation by Rubisco (μmol CO_2 m^{-2} s^{-1}), k_c and k_o are the Michaelis coefficients for carboxylation and oxygenation of Rubisco respectively (dimensionless), r_d is the rate of respiration in the light attributed to processes other than photorespiration (μmol CO_2 m^{-2} s^{-1}), and o_i is the oxygen concentration (ppm).

The rate of photosynthesis dependent upon the light-limited rate of ribulose bisphosphate (RuBP) regeneration, A_i, depends on the rate of electron transport, J (μmol electrons m^{-2} s^{-1}), as:

$$A_i = \frac{\gamma J C_i}{4(C_i + o_i/\tau)} - r_d, \tag{6}$$

where τ is the specificity factor of Rubisco for CO_2 relative to O_2, and J is dependent upon irradiance, q (μmol PAR m^{-2} s^{-1}), and the rate of light-saturated electron transport, J_m (μmol electrons m^{-2} s^{-1}), as:

$$J = \frac{\alpha q J_m}{\sqrt{\alpha^2 q^2 + J_m^2}}, \tag{7}$$

where α is the efficiency of light conversion (0.18 mol electrons/mol photons) (Harley et al., 1992). Values of k_o and k_c have the general temperature dependences given by Harley et al. (1992). The temperature dependencies of V_m and J_m below 25 °C are given by Long (1991) and above 25 °C by Beerling and Woodward (2001). If V_{cmax} and J_{max} (μmol m^{-2} s^{-1}) are the values of V_m and J_m at 25 °C, then V_{cmax} is a parameter to be determined by experiment, and $J_{max} = 1.64V_{cmax} + 29.1$ (Wullschleger, 1993) (μmol m^{-2} s^{-1}).

2.3. Modelling C_i and liverwort CO_2 supply as functions of C_a

Obtaining $\delta^{13}C_p$ as a function of C_a (Eq. (1)) requires C_i as a function of C_a which is given by rearrangement of Eq. (2). Eq. (2) models the flux of CO_2 from the atmosphere into the thallus by analogy with Ohm's Law. The difference $C_a - C_i$ between the external and internal CO_2 partial pressures plays the role of a potential difference driving the flow, with the photosynthesis rate A being a CO_2 sink term representing the 'current' or rate of gas flow into the thallus. The constant of proportionality between these two is the resistance r.

A as a function of C_i is given by Eqs. (5) (for Rubisco-limitation) and (6)–(7) (for light-limitation). On substituting these functions into (2) and rearranging, we find that C_i satisfies the quadratic equation

$$C_i^2 + \left(rV_m - [rr_d + C_a] + k_c 1 + \frac{o_i}{k_o}\right)C_i - \left(\frac{ro_i V_m}{2\tau} + [rr_d + C_a]k_c 1 + \frac{o_i}{k_o}\right) = 0, \tag{8}$$

for the Rubisco-limited case, or

$$4C_i^2 + \left(rJ - 4[rr_d + C_a] + \frac{4o_i}{\tau}\right)C_i - \left(\frac{ro_i J}{2\tau} + [rr_d + C_a]\frac{4o_i}{\tau}\right) = 0, \tag{9}$$

for the light-limited rate of electron transport case. The positive roots of these equations are the candidates for C_i, namely:

$$C_i = \frac{-w + \sqrt{w^2 - 4x}}{2}, \tag{10}$$

where:

$$w = rV_m - (rr_d + C_a) + k_c\left(1 + \frac{o_i}{k_o}\right), \tag{11}$$

and:

$$x = -\left(\frac{ro_i V_m}{2\tau} + (rr_d + C_a)k_c\left(1 + \frac{o_i}{k_o}\right)\right), \quad (12)$$

for the Rubisco-limited case, or

$$C_i = \frac{-y + \sqrt{y^2 - 16z}}{8}, \quad (13)$$

where:

$$y = rJ - 4(rr_d + C_a) + \frac{4o_i}{\tau}, \quad (14)$$

and

$$z = -\left(\frac{ro_i J}{2\tau} + (rr_d + C_a)\frac{4o_i}{\tau}\right), \quad (15)$$

for the light-limited rate of electron transport case, the final value of C_i chosen being the one that gives the smallest photosynthesis rate when substituted back into Eq. (5) or (6) (for the solution of Eq. (10) or (13), respectively).

It remains to specify the resistance r. For this we use the following linear function of C_a:

$$r = 0.013C_a + 27. \quad (16)$$

Eq. (16) (Fig. 2 upper panel) was obtained by iteration, as follows. A first guess at the slope and offset were used to fit the physiological parameters V_{cmax} and r_d as per Section 2.4 below. A set of measurements of rA, at different values of C_a, independent of the photosynthesis measurements used to fit V_{cmax} and r_d (Fletcher et al., 2005) provide a crosscheck on Eq. (16) (Fig. 2 middle panel). Eqs. (5)–(7) were used, via Eqs. (8) and (9), to calculate values of A at the C_a values in question, and the results divided into the measured rA values to give 'measured' values of the resistance r, which compared favourably ($R^2 = 92.5\%$, $n = 18$, $P < 0.001$) with the values as given by Eq. (16).

2.4. Method of calculation

2.4.1. Photosynthesis parameters

From the A/C_a measurements (Section 3; Fig. 3), and given r as a function of C_a (Eq. (16)), the parameters describing A as a function of C_i can be fitted to the (A, C_a) data pairs because we now have C_i as a function of C_a (Eqs. (8) and (9)). We included the constraint $r_d \geqslant V_{cmax}/100$ as r_d is approximately an order of magnitude lower than A (note that in Section 2.1 it was treated as being a fixed fraction, 0.06, of A). If r_d was treated as a free parameter the least squares fit gave an unrealistic negative value for r_d. Our procedure gives $r_d = 0.34$ μmol m^{-2} s^{-1} and $V_{cmax} = 34$ μmol m^{-2} s^{-1}. Crosschecking indicated that the fully coupled photosynthesis-isotope model adequately explained the response of $\Delta^{13}C$ displayed by the original dataset (Fig. 2, lower panel).

2.4.2. For given environmental conditions

Given a set of environmental parameters (atmospheric CO_2 and O_2 concentrations, irradiance and temperature)

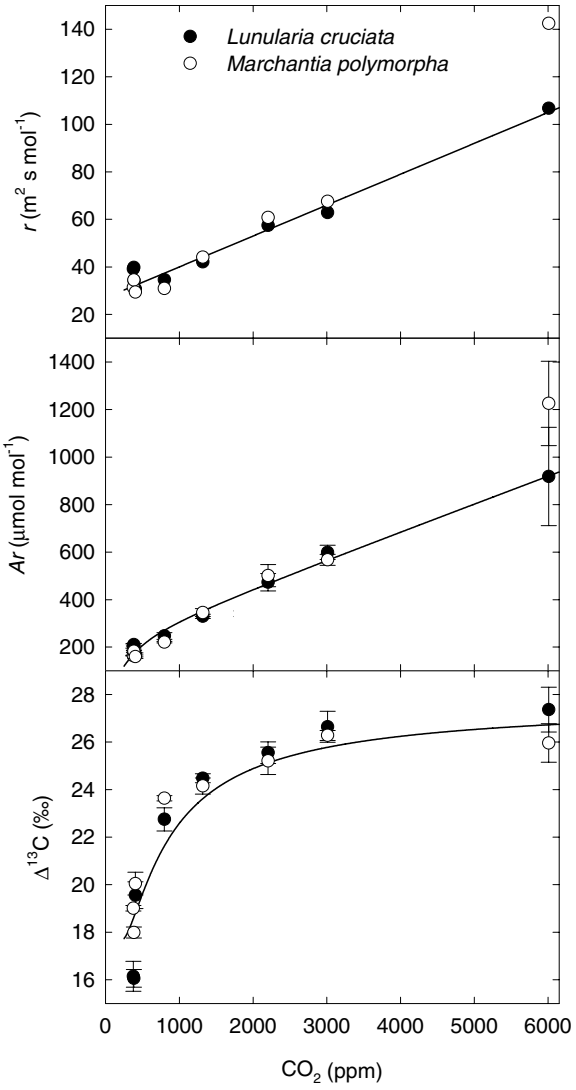

Fig. 2. Effect of growth CO_2 concentration on (top) resistance, (middle) [photosynthesis × resistance] or [$C_a - C_i$], and (bottom) discrimination against ^{13}C ($\Delta^{13}C$). Data points in the top two panels are calculated from those in the bottom panel, and lines are the model best fit.

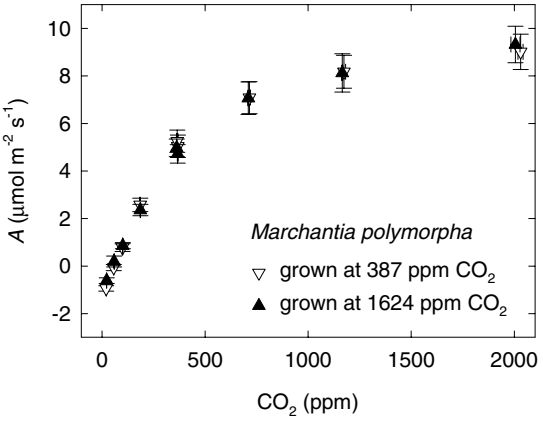

Fig. 3. The response of photosynthesis (A) to variations in atmospheric CO_2 (C_a) in *Marchantia polymorpha* grown at two atmospheric CO_2 concentrations. Data are means ± standard error ($n = 3$ plants).

and our fitted physiological parameters V_{cmax} (hence J_{max}) and r_d, we first calculate the CO_2 concentration inside the thallus, C_i using Eqs. (8) and (9), as described above. This value is then substituted into Eq. (1) to give the predicted value of $\delta^{13}C_p$; this requires knowledge of the corresponding atmospheric value $\delta^{13}C_a$, which is either measured in experiments, or obtained from the marine carbonate record. Isotopic discrimination is calculated as given in Eq. (4). See Appendix A for the calculation procedure required to determine atmospheric CO_2 concentration from $\Delta^{13}C$.

3. Gas exchange and $\Delta^{13}C$ measurements

We calculated V_{cmax} (and hence J_{max}) and r_d for BRYOCARB from a series of CO_2 assimilation measurements on liverworts grown in conditions similar to those described previously (Fletcher et al., 2005). *Marchantia polymorpha* L. was propagated from gemmae collected from the University of Sheffield Tapton Experimental Gardens. Gemmae were sown on pots of moist potting compost and grown for 6 weeks in a pair of controlled environment cabinets (Conviron, Winnipeg, Canada) providing 200 ± 10 μmol light $m^{-2} s^{-1}$ for 12 h per day, at 20 °C, 75% RH, and either 387 or 1624 ppm CO_2 (Ciras-1 IRGA, PP Systems). Plants and their associated CO_2 settings were rotated between cabinets once a week.

Photosynthesis was measured on ~4 cm^2 of detached thallus, rinsed in distilled water and blotted dry, and placed in a Parkinson narrow leaf cuvette (PLC) (PP Systems, Hoddesdon, UK) connected to a portable infra-red gas analyzer (Ciras-1) housed in a controlled environment cabinet (Fig. 3). Photosynthesis–CO_2 response curves were constructed by making measurements by decreasing CO_2 progressively from 400 ppm down to 20 ppm, and then increasing it from 400 ppm up to 2000 ppm. Gas exchange parameters were measured every 5 min when steady-state fluxes were evident at 20 ± 1 °C with 250 ± 5 μmol PAR $m^{-2} s^{-1}$. Measurements were then corrected for area as determined by an area meter mk2 (Delta-T devices, Cambridge, UK). Measurements are the mean of three thalli. Bulk thallus nitrogen content of dried, ground *M. polymorpha* and *Lunularia cruciata* (L.) Dum. ex Lindb grown at both CO_2 concentrations was determined with an isotopic ratio mass spectrometer (ANCA GSL preparation module, 20–20 stable isotope analyser, PDZ Europa, Cheshire, UK).

Measurements of the response of thallose photosynthetic rate were conducted as described above on 1-year-old populations of *M. polymorpha* and *L. cruciata* grown outdoors on pots of sand and vermiculite (3:2) at Tapton Experimental Gardens. Measurements were made on approximately 1–2 cm^2 of thallus at a range of irradiances, temperatures and O_2 levels. Temperature and O_2 measurements were conducted at light-saturating levels of 200 μmol PAR $m^{-2} s^{-1}$ for *L. cruciata* or 600 μmol PAR $m^{-2} s^{-1}$ for *M. polymorpha*. Temperature and irradiance were controlled by the controlled environment cabinet, C_a by the IRGA, and O_2 by supplying N_2 and O_2 (BOC gases, Surrey, UK) mixed by mass-flow controllers (Brooks instruments B. V., Veenendaal, Holland).

To test BRYOCARB predictions of the effect of light and CO_2, both separately and interactively, on $\Delta^{13}C$ *L. cruciata* and *M. polymorpha* were grown at two CO_2 levels and a range of irradiances in a factorial experiment with 5 plants per treatment. Growth conditions were as described above, with growth cabinets supplying 398 ppm (ambient) or 791 ppm (elevated) CO_2, and 400, 200, 100 or 50 μmol PAR m^{-2} provided by varying the distance between the lamps and the plants, and shading some with reflective scrim (Lee filters, Andover, UK). Whole-plant $\delta^{13}C$ was measured on bulk organic matter after six weeks' growth using the same instrument (PDZ Europa) as before. $\delta^{13}C_a$ was measured four times during the course of a single representative day, giving $\delta^{13}C_a$ of −9.0‰ in the ambient CO_2 cabinet and −21.2‰ in the elevated CO_2 cabinet. We employed a simple mass-balance calculation to provide an additional cross-check on the elevated $\delta^{13}C_a$ measurement, constrained by measuring the $\delta^{13}C_a$ of CO_2 in the ambient treatment and pure CO_2 from the cylinders:

$$\delta^{13}C_{elevated} = \left(\frac{[CO_2]_{ambient}}{[CO_2]_{elevated}} \cdot \delta^{13}C_{ambient}\right) + \left(\frac{[CO_2]_{elevated} - [CO_2]_{ambient}}{[CO_2]_{elevated}} \cdot \delta^{13}C_{cylinder}\right), \quad (17)$$

which gave the $\delta^{13}C_a$ in the elevated treatment as −22.9‰, reasonably close to the measured value.

To test BRYOCARB modelled response of $\Delta^{13}C$ to O_2, *M. polymorpha* was grown for six weeks in 4-L Perspex growth chambers ($n = 5$ per O_2 concentration), supplied with pressure-regulated compressed air (control: 21% O_2, 404 ppm CO_2), or air mixed with O_2 and 5% CO_2 in air (elevated O_2: 30 ± 1% O_2, 402 ppm CO_2) (BOC gases, Surrey, UK) by mass-flow controllers as described previously (Fletcher et al., 2005). Needle valves regulated a 500 ± 50 ml min^{-1} air supply to each chamber. The chambers were housed in a laboratory flow hood fitted with 400 W lamps (Metalarc HSI metal halide lamps, Sylvania, Shipley, UK) providing 196 ± 50 μmol PAR $m^{-2} s^{-1}$ for 18 h per day, at 24 °C (PAR sensor, Skye Instruments, Powys, UK; Squirrel datalogger, Grant Instruments, Cambridgeshire, UK). All gas exchange and $\delta^{13}C$ measurements were carried out as described above. $\delta^{13}C_a$ was −8.8‰ in the control, and −10.6‰ in the elevated oxygen treatment. A simple mass-balance calculation was used to provide an additional check on the elevated-O_2 $\delta^{13}C_a$ measurement, constrained by measuring the $\delta^{13}C_a$ of CO_2 in the ambient O_2 treatment, and CO_2 from the 5% CO_2 cylinder:

$$\frac{[CO_{2\ \text{elevated}}] - \left(\frac{100-\%O_{2\ \text{elevated}}}{100-\%O_{2\ \text{control}}} \cdot [CO_{2\ \text{control}}]\right)}{[CO_{2\ \text{elevated}}]} \cdot \delta^{13}C_{\text{cyclinder}} + \frac{\left(\frac{100-\%O_{2\ \text{elevated}}}{100-\%O_{2\ \text{control}}} \cdot [CO_{2\ \text{control}}]\right)}{[CO_{2\ \text{elevated}}]} \cdot \delta^{13}C_{a\ \text{control}}, \quad (18)$$

which estimated air in the elevated O_2 treatment as $-10.9‰$, close to that of the measured value.

We conducted an isotopic survey of three rural garden populations of liverworts by making paired $\delta^{13}C$ measurements of bulk organic matter and air to estimate $\Delta^{13}C$ and test the utility of BRYOCARB for predicting $\Delta^{13}C$ in natural habitats rather than controlled environment conditions. Bulk organic matter was analyzed from five *L. cruciata* individuals from each population of three suburban garden sites in Sheffield, UK (Table 1). $\delta^{13}C_a$ was measured close to the ground surface at the growth site in a morning and an afternoon (5 replicate measurements each time interval). The degree of shading was assessed by spot-measuring PAR on at least three parts of the patch of liverworts as well as incident PAR in the open.

4. Results and discussion

4.1. Simulating liverwort photosynthesis in response to environmental change

We simulated changes in photosynthetic CO_2 assimilation with BRYOCARB and evaluated the results against measurements made on two species of field-grown liverworts (*M. polymorpha* and *L. cruciata*). Photosynthesis measurements were made under a range of irradiances, atmospheric O_2 concentrations and temperatures, at two CO_2 concentrations.

The model accurately simulates the light-response of photosynthesis at atmospheric CO_2 concentrations of 400 and 1000 ppm, in agreement with our measurements (Fig. 4 upper panel) and previous observations (Green and Snelgar, 1983; Marschall and Proctor, 2004). Simulated light-saturated photosynthesis rates of ~2 μmol CO_2 m^{-2} s^{-1} at 400 ppm CO_2 increased to 3 μmol CO_2 m^{-2} s^{-1} at 1000 ppm CO_2, with rates slightly higher in *M. polymorpha* than in *L. cruciata*. These rates of photosynthesis are consistent with V_{cmax} values lower than those of laboratory-grown populations; $V_{cmax} = 8$ μmol CO_2 m^{-2} s^{-1} for *L. cruciata* and 8.5 μmol CO_2 m^{-2} s^{-1} for *M. polymorpha*.

Table 1
Ground level light, $\delta^{13}C_a$, and *Lunularia cruciata* $\Delta^{13}C$ in semi-rural Sheffield gardens

Site	Light (% PAR in open)	$\delta^{13}C_a$ (‰)	$\Delta^{13}C$ (‰)
Overgrown gravel path	35 ± 3.5	−9.2 ± 0.2	21.7 ± 0.1
Turf on shady bank	8 ± 7	−11.1 ± 0.5	19.5 ± 0.3
Turf under hedge	6 ± 6	−10.8 ± 0.7	21.0 ± 0.1
Mean	16 ± 9	−10.3 ± 0.6	20.7 ± 0.6

Data are ± standard error.

The slope of the response of A to irradiance defines the quantum efficiency (α) and implies a value of 0.1 rather than 0.18 used in the generalized BRYOCARB model, an observation consistent with a low photosystem II efficiency in liverworts (Gimeno and Deltoro, 2000). For mosses, the leaf and shoot structures can reduce light absorption giving even lower α values of 0.04–0.015 (Swanson and Flanagan, 2001; Williams and Flanagan, 1998).

Simulations of the photosynthetic response to O_2 shows the expected inhibition that occurs as O_2 out-competes CO_2 for the active binding site in the acceptor molecule RuBP and leads to catalysis of the oxygenation reaction by Rubisco and release of CO_2 (i.e., photorespiration) (Lawlor, 1993). The simulated responses of A to O_2 are in close agreement with measurements made on both liverwort species (Fig. 4, middle panels) and are consistent with earlier observations on bryophytes (Green and Lange, 1995) and vascular plants (Beerling et al., 2002). The model also accurately captures the suppression of O_2-driven photorespiration in a CO_2-enriched atmosphere (Fig. 4, right middle panel).

The generalized temperature responses of photosynthetic physiology within BRYOCARB allow it to account for the effect of temperature on A. This occurs largely by altering the relative solubility of CO_2 and O_2 and the specificity of Rubisco for CO_2 (Lawlor, 1993). Photosynthesis (A) is simulated to increase from 15 °C towards an optimum around 25 °C, above which it then declines. Measurements of A show a similar pattern, with those of *M. polymorpha* reaching an optimum ~25 °C and of *L. cruciata* of ~20 °C (Fig. 4, lower panels). The strong synergistic effect of temperature in high CO_2 seen in bryophytes (Fig. 4) and vascular plants (Long, 1991) is also reproduced in the simulations. This effect results from the suppression of oxygenation by high CO_2 and can raise the optimum temperature for A (Long, 1991), as shown by measurements on *L. cruciata* and to a lesser extent *M. polymorpha* (Fig. 4, middle panels). Although BRYOCARB captures the response of liverwort A to temperature and its interaction with CO_2, modelled A rates are compared to observations either too low in the case of *M. polymorpha* or too high in the case of *L. cruciata*. The fit-to-data could clearly be improved by developing species-specific temperature response functions for A, but this is not an aim of the current model.

The different temperature optima for photosynthesis in *M. polymorpha* and *L. cruciata* at ambient CO_2 may help explain earlier apparently contradictory responses of $\Delta^{13}C$ to a 4 °C warming in these species. In a laboratory experiment, Fletcher et al. (2005) showed that $\Delta^{13}C$ in *M. polymorpha* decreased by ~0.4‰ per °C in response to a 4 °C warming, whereas in *L. cruciata* it increased by approximately 0.2‰ per °C. For *M. polymorpha* with a temperature optimum of 25 °C, a 4 °C increase above 20 °C increases photosynthesis, decreasing C_i, C_i/C_a and $\Delta^{13}C$. In contrast, for *L. cruciata* the additional warming of 4 °C reduces photosynthetic rates, increasing C_i, C_i/C_a and $\Delta^{13}C$ (Fletcher et al., 2005).

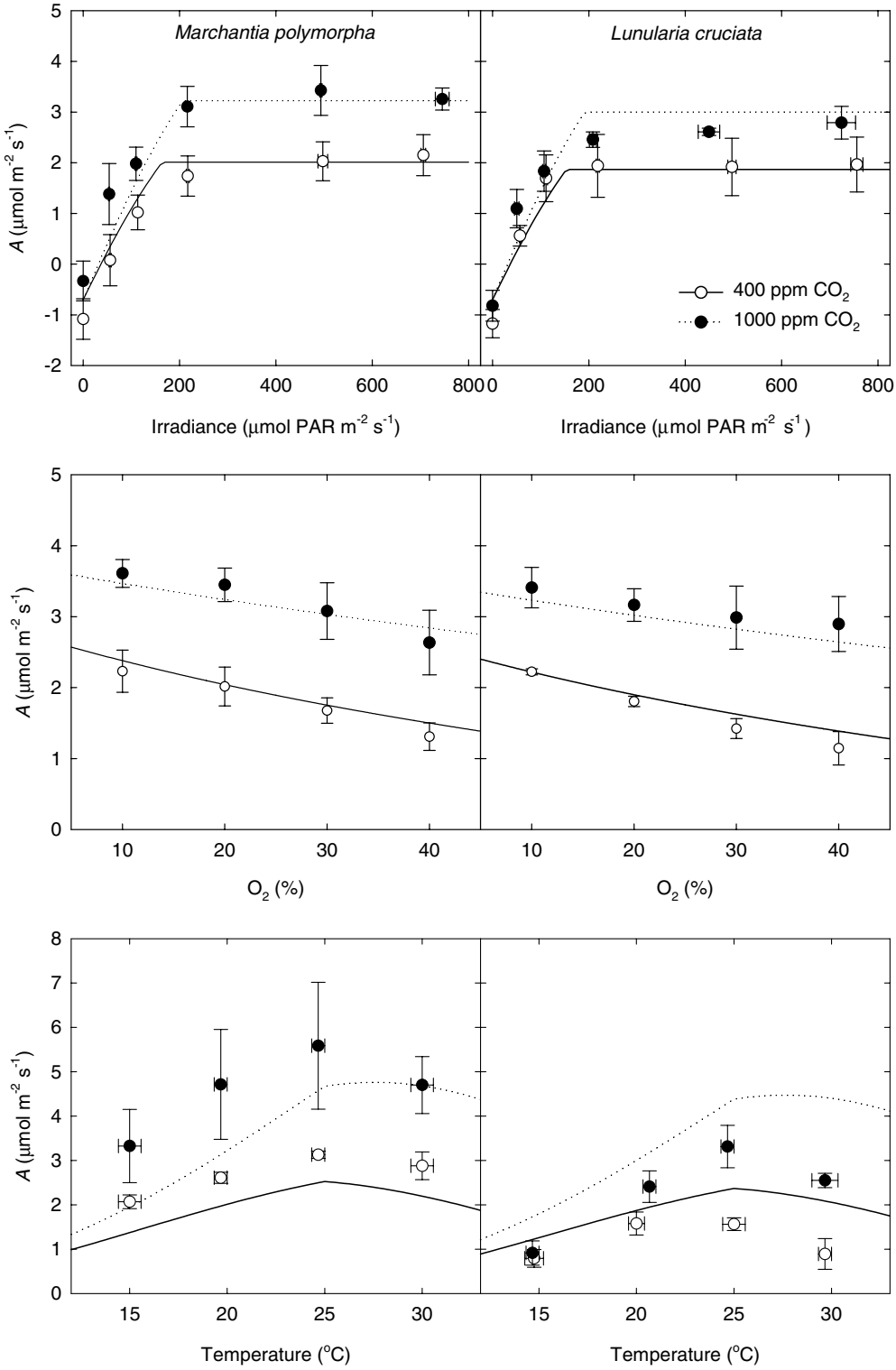

Fig. 4. Effects of irradiance (top), atmospheric O_2 (middle), and temperature (bottom) on the photosynthetic rates of two liverworts measured at two CO_2 concentrations. Points indicate measurements, lines indicate model fit. Measurement data are means ± standard error ($n = 3$ plants).

Overall, these results indicate that BRYOCARB accurately describes the balance between CO_2 demand by the thallose photosynthetic tissues and the resistance to its supply from the atmosphere under a wide variety of environmental conditions. It is therefore assumed that we can predict C_i with reasonable confidence for a given set of conditions (Section 2.3). This establishes a secure basis for investigating how possible variations in physiology and

environmental conditions may influence the critical dependency of $\Delta^{13}C$ on CO_2, which underpins the potential for bryophytes to act as a CO_2 proxy.

4.2. Sensitivity of BRYOCARB to variations in photosynthetic physiology

One of the main determinants of liverwort CO_2 assimilation under a given set of environmental conditions is the maximum rate of carboxylation by Rubisco (V_{cmax}) (Eq. (5)). We calculate a value for *M. polymorpha* (34 μmol m^{-2} s^{-1}) matching that determined from the A–C_a response reported by Griffiths et al. (2004), given 411 mg chlorophyll m^{-2} (B. Fletcher, unpublished) and our estimates of r and r_d. These V_{cmax} values are at the low end of the range (6–194 μmol m^{-2} s^{-1}) of vascular plants (Wullschleger, 1993) and imply a low investment of nitrogen in Rubisco. This is supported by the relatively low nitrogen contents of *M. polymorpha* and *L. cruciata*, 1.3 and 1.2 mmol g^{-1}, respectively, compared to vascular plants (0.5–5.0 mmol g^{-1}; Field and Mooney, 1986).

However, V_{cmax} determinations from A–C_a responses of field populations of *M. polymorpha* and *L. cruciata* indicate values can be as low as ~8 μmol m^{-2} s^{-1}, suggesting a degree of phentotypic plasticity in this feature of bryophytes. We therefore assessed the influence of variations in V_{cmax} such as may be caused by adaptation, interspecific differences or evolutionary change over geologic time. According to our simulations, if V_{cmax} (and hence J_{max}) is increased, A rises (Fig. 5, upper left panel), depleting internal CO_2 and decreasing $\Delta^{13}C$ (Fig. 5, upper right panel). Doubling V_{cmax} decreases $\Delta^{13}C$ by ~0.9‰; halving V_{cmax} increases it by ~1.2‰ and by slightly more below 600 ppm, as V_{cmax} now further limits A, increasing C_i. Variations in r_d exerted generally minor effects on A and $\Delta^{13}C$ (Fig. 5, lower left panels). Doubling it increased $\Delta^{13}C$ by <1‰ at 400 ppm and <0.4‰ above 1000 ppm, decreasing it had a even smaller effect; with r_d at one-tenth the fitted value, $\Delta^{13}C$ is only <0.3‰ lower. The very small effect of changes in r_d is mainly due to the re-fractionation of already fractionated respired CO_2; respired CO_2 being diluted at higher external CO_2 levels.

Based on these analyses, uncertainties in the photosynthetic physiology of liverworts in the past may exert minor effects on the dependency of $\Delta^{13}C$ on CO_2. Although this suggestion is supported by the similar response of the two species grown across a wide range of CO_2 concentration, it requires further investigation. Furthermore, we found no evidence of down-regulation in the maximum rate of carboxylation (V_{cmax}) or differences in nitrogen content of *M. polymorpha* when grown under elevated CO_2, responses often seen in vascular land plants cultivated in a CO_2-enriched atmosphere (Long et al., 2004). This suggests the nitrogen investment in the photosynthetic proteins by liverworts in the geologic past when atmospheric CO_2 was higher may not have been markedly different from now.

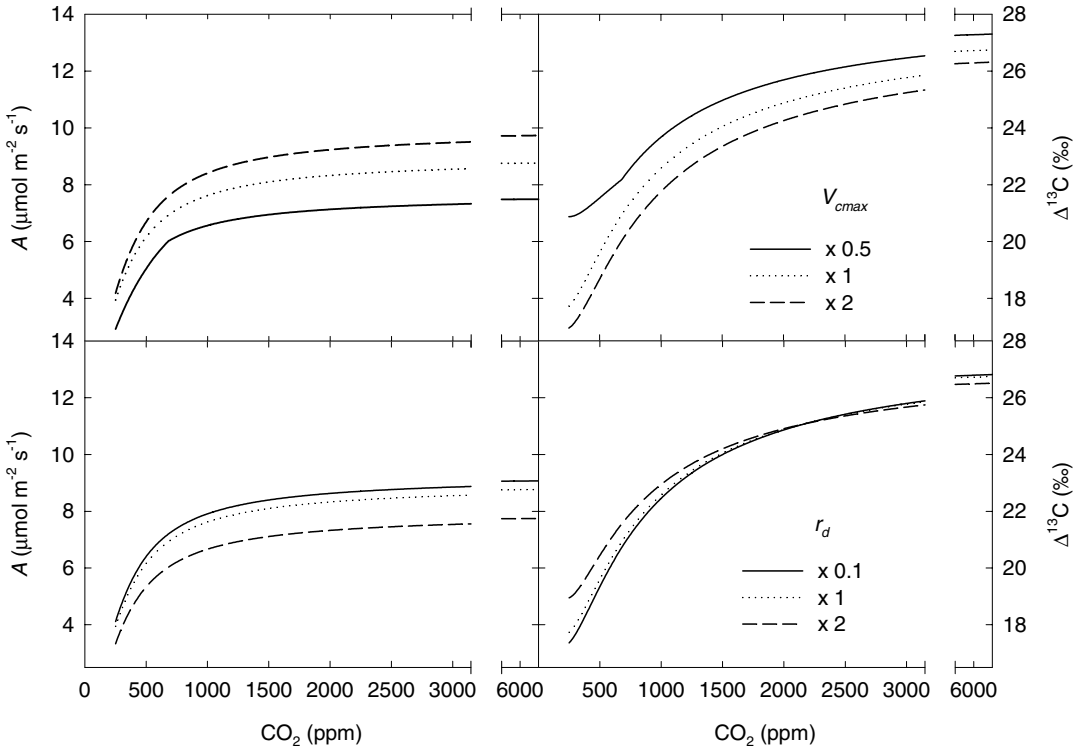

Fig. 5. Sensitivity of the modelled photosynthesis (A) and $\Delta^{13}C$ to changes in photosynthetic physiology. Two parameters of the model fit to experimental data (dotted lines) were changed: (top) maximum rate of carboxylation (V_{cmax}) × 0.5 (solid line) and × 2 (dashed line), and (bottom) dark respiration rate × 0.1 (solid line) and × 2 (dashed line).

4.3. Simulated sensitivity of $\Delta^{13}C$ dependency on CO_2 to temperature, irradiance and O_2

We examined the simulated sensitivity of liverwort organic matter $\Delta^{13}C$ to the same three environmental variables used in our gas exchange analyses (O_2, temperature and irradiance) to determine their potential to influence the dependency of $\Delta^{13}C$ on CO_2 and compared the results with those from experiments and field surveys.

In growth experiments, $\Delta^{13}C$ in *M. polymorpha* at 400 ppm atmospheric CO_2 increased by 1.1‰ (Fig. 6, upper panel) between 21% and 30% O_2, a range representative of that likely experienced by plants during the Phanerozoic (Berner, 2001) (Fig. 9, middle panel). In order to simulate this response, we determined the V_{cmax} for plants grown at the two O_2 levels (Fig. 6, lower panel). Utilizing these values of V_{cmax}, allowed BRYOCARB to closely reproduce the observed increase (+1.0‰; Fig. 6, upper panel) caused by increasing rates of photorespiration, the reduction of photosynthetic CO_2 fixation by competitive O_2 fixation (Fig. 6, subplot) (Section 4.1). Additionally, photorespiration due to high O_2 has an isotopic effect increasing the apparent $\Delta^{13}C$, as C is re-fractionated (Gillon and Griffiths, 1997). Further simulations with BROCARB indicate the effect of rising O_2 on $\Delta^{13}C$ is diminished at higher CO_2 concentrations (Fig. 6, upper panel) because of the suppression of photorespiration, as observed in red algae (Kübler et al., 1999) and vascular plants (Berner et al., 2000; Beerling et al., 2002).

The simulated effect of a warming of 10 °C, the approximate mean global range through the Phanerozoic (Fig. 9, lower panel), is small. In contrast to the effects of O_2, the effect of variation in temperature on A is minimal at low CO_2 but greater at high CO_2 (Fig. 7, upper panel). At low CO_2 (<500 ppm), increasing the temperature from 15 to 25 °C slightly decreases A, by lowering the specificity of Rubisco for CO_2 relative to O_2, thus favouring the competitive oxygenation reaction. At higher CO_2, oxygenation is sufficiently suppressed to allow the kinetic effects of increasing temperature to increase A. Small differences in physiological variables shift the CO_2 level at which this changeover occurs (compare Fig. 4, bottom panel, model, where, at 400 ppm, A increases from 15 to 25 °C), but as the effect on $\Delta^{13}C$ of this 10 °C range is quite small,

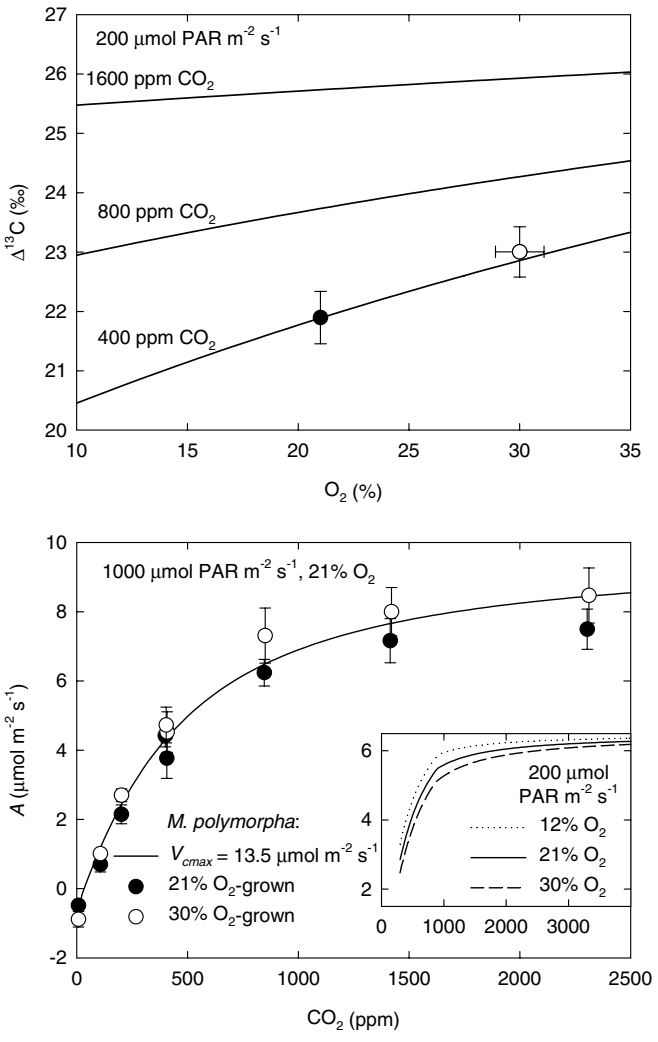

Fig. 6. Sensitivity of the dependency of photosynthesis (A) and $\Delta^{13}C$ on CO_2 in *M. polymorpha* in response to changes in atmospheric O_2. Measurements of $\Delta^{13}C$ (upper panel, points) and gas exchange at saturating irradiance, allowing accurate determination of V_{cmax}, (lower panel) made on plants grown at 400 ppm CO_2 and 21 or 30% O_2. This V_{cmax} was used to simulate A (inset) and $\Delta^{13}C$ (upper panel, lines) at growth irradiance.

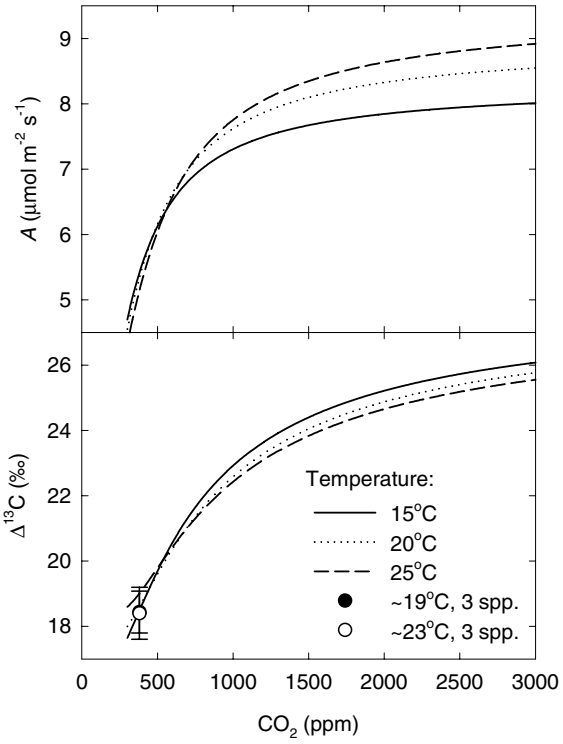

Fig. 7. Simulated sensitivity of the dependency of photosynthesis (A) and $\Delta^{13}C$ on CO_2 in response to three different temperatures. Also shown (lower panel) are the average (±SE) $\Delta^{13}C$ responses of 3 species calculated from earlier $\delta^{13}C_p$ measurements (Fletcher et al., 2005) and $\delta^{13}C_a$ of −10.3‰ (Table 1).

<0.6‰ above 375 ppm (Fig. 7, upper panel), this is a relatively minor source of error. This is in agreement with earlier measurements on three liverwort species (Fletcher et al., 2005) over a 4 °C increase, in which $\Delta^{13}C$ ($\delta^{13}C_a$ value from Table 1) increased by <0.1‰ on average (Fig. 7, lower panel).

The influence of irradiance on the relationship between $\Delta^{13}C$ and CO_2 was investigated by growing *M. polymorpha* and *L. cruciata* at two CO_2 levels and a wide range of light levels (Fig. 8, middle panels), bracketing those typically experienced by liverworts in the field (Fig. 8, lower panel). The observed interaction between CO_2 and irradiance on $\Delta^{13}C$ in two species of liverworts is in general agreement with that predicted by BRYOCARB (Fig. 8). In the model, $\Delta^{13}C$ is reduced between the extreme low and high irradiances by 8.5‰ at 400 ppm CO_2 to 7.9‰ at 800 ppm CO_2 and by ⩽4‰ at high CO_2 (>3300 ppm CO_2). However, observed reductions in $\Delta^{13}C$ between the extreme low and high irradiances are smaller, 6.5–6.4‰ in *L. cruciata* and 5.8–4.8‰ in *M. polymorpha*, which may indicate a degree of photosynthetic acclimation. The modelled direction of change in $\Delta^{13}C$, but not the magnitude, is also consistent with observations on the moss *Tortula ruralis* showing $\Delta^{13}C$ decreased by 2‰ between a shade (50–250 μmol PAR $m^{-2}\,s^{-1}$) and sun (150–900 μmol PAR $m^{-2}\,s^{-1}$) at a field site (Hamerlynck et al., 2002).

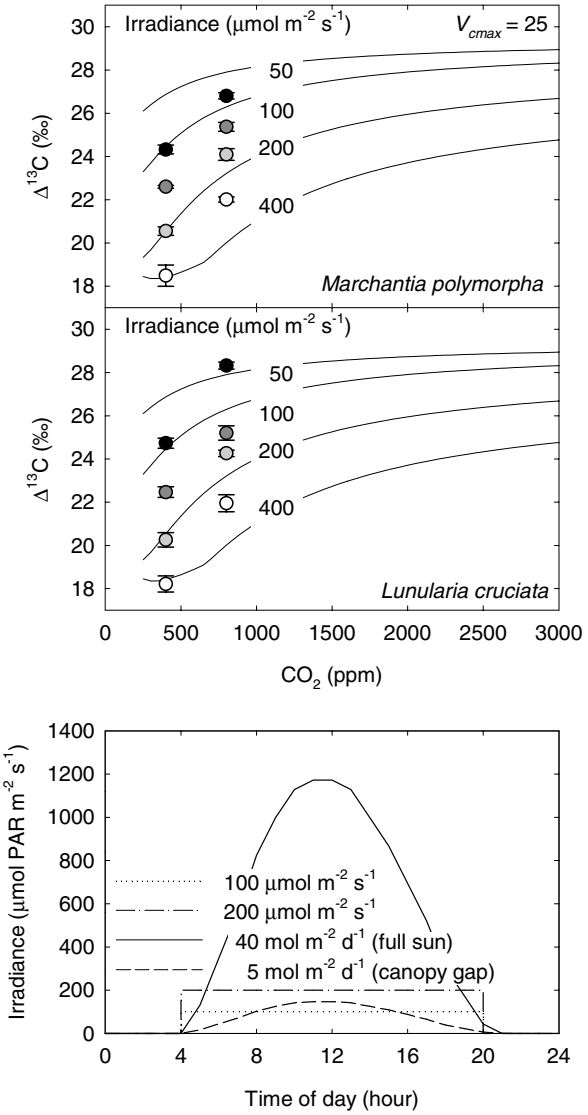

Fig. 8. Sensitivity of the dependency of $\Delta^{13}C$ on CO_2 in response to changes in irradiance. Simulated $\Delta^{13}C$ response (upper and middle panels, lines) derived from the model fit, with a V_{cmax} of 25, to observed $\Delta^{13}C$ at 400 and 800 ppm CO_2 (upper and middle panels, points). Irradiance levels used in the experiments (mean ± s.e., $n = 5$) represent varying degrees of shading of average incident summer sunlight (lower panel, solid line) (Mitchell, 1992), and include light levels well above and below typical field settings such as gaps in midsummer woodland canopy (lower panel, dashed line), (Mitchell, 1992).

We emphasize that although irradiance exerts a strong influence on $\Delta^{13}C$, the range employed in our experiments likely exceeds that experienced in the field. Observations around the Sheffield region on sunny days suggest that liverworts usually occupy partially shaded sites with 150–250 μmol PAR $m^{-2}\,s^{-1}$ or lower; less shaded growth sites experiencing ~350 μmol PAR $m^{-2}\,s^{-1}$ (~30% full sun) (Mitchell, 1992; B. Fletcher, unpublished). Another difference between the experiments and field conditions is that in the latter situation, the quantity of PAR varies through the day (Fig. 8, lower panel). The southern UK (~52°N) receives on average ~40 mol PAR $m^{-2}\,d^{-1}$ incident light at midsummer, equating to midday values ~1200 μmol PAR $m^{-2}\,s^{-1}$ when integrated over the course of a day. Riparian woodland margins, locations commonly colonized by liverworts, typically receive ~5 mol PAR $m^{-2}\,d^{-1}$ (i.e., ~88% shading; Mitchell, 1992), equating to midday values ~150 μmol PAR $m^{-2}\,s^{-1}$ given the same distribution through the day (Fig. 8). As relatively more carbon will be fixed around midday due to the higher light and warmer temperatures, typical midday irradiance values of ~150–250 μmol $m^{-2}\,s^{-1}$ provide a closer approximation to that suitable for simulating $\Delta^{13}C$. Indeed, additional variation caused by the movement of the sun casting shade or sunflecks at different times of the day, and variation in cloud cover, make accurate *A* rate-weighted integration of $\Delta^{13}C$ over the course of a growing season impractical.

These analyses suggest that variation in irradiance rather than O_2 or temperature is the most likely environmental factor confounding any CO_2 signal preserved in fossil liverwort specimens. Water availability has a large effect on moss, but not liverwort $\Delta^{13}C$. This is thought to be because liverworts grow where a relatively constant water content can be maintained, whilst mosses conduct large amounts of water externally in wet conditions, leading to large variations in *r* and hence *A* and $\Delta^{13}C$ (Fletcher et al., 2005, and references therein).

4.4. Field survey

In our survey of the isotopic composition of field-grown populations and atmospheric CO_2, we found $\delta^{13}C_a$ to be

2.2‰ more negative than the value of −8.1‰ measured at the Pacific island of Mauna Loa in 2002 (see http://cdiac.esd.ornl.gov/trends/co2/iso-sio/data/iso-data.html). The offset may reflect isotopically light soil respired CO_2, and/or a partial contribution from anthropogenic CO_2 emissions. The paired organic matter and $CO_2\delta^{13}C$ measurements gave a $\Delta^{13}C$ for field-grown plants of 20.7 ± 0.6‰, a value that closely matches the model prediction of 20.1‰ at 200 μmol PAR m^{-2} s^{-1}. This is consistent with the use of irradiance values 80–90% below mean summer midday irradiances to calculate $\Delta^{13}C$ for field plants, as 200 μmol PAR m^{-2} s^{-1} corresponds to an incident irradiance of 1200 μmol PAR m^{-2} s^{-1} (Fig. 8; Mitchell, 1992) with 84% shading at the growth sites (Table 1).

Assuming $\delta^{13}C_a$ in field situations to be 1.98‰ more negative than in pristine air above the Pacific ocean yields a mean $\Delta^{13}C$ ($n = 25$ measurements, 8 species) for a compilation of thallose liverworts in the field (Fletcher et al., 2004; Fletcher et al., 2005) of 19.6 ± 0.5‰. The close agreement, within 0.5‰ of the model, suggests BRYOCARB captures the 'average' value of field populations across a range of species.

4.5. Simulated variations in liverwort $\Delta^{13}C$ through the Phanerozoic

We used BRYOCARB to simulate the separate and combined effects of Phanerozoic (up to 542 million years ago [Ma]) changes in CO_2 (Berner and Kothavala, 2001), O_2 (Berner, 2001) and temperature on liverwort $\Delta^{13}C$ (Fig. 9) to assess the likely departure expected in fossil materials compared to modern plants. Global temperature change through the Phanerozoic (Fig. 9, lower panel) was calculated by modifying a simple zero-dimensional model of planetary energy balance that collapses latitude, altitude and longitude to give a single global mean value for a given atmospheric CO_2 concentration (Beerling and Woodward, 2001). These calculations include the effects of CO_2, via the atmospheric greenhouse effect, and the effect of the estimated ~5% increase in the Sun's output over the past 500 Myr (Caldeira and Kasting, 1992). The model was run with the experimentally determined V_{cmax} of 34.0, and an estimated average V_{cmax} of $21.7 + 6.5/-1.6$ derived from natural populations of liverworts.

Variations in O_2 influenced $\Delta^{13}C$ most strongly during the rise in the Permo-Carboniferous (359.2–251 Ma), and from the Cretaceous onwards (145.5–0 Ma) by depressing A through increased photorespiration (Fig. 10, upper left). This increased C_i and therefore C_i/C_a and $\Delta^{13}C$ by ~4‰ in the Permian (299–251 Ma) and ~2‰ in the Late Cretaceous (99.6–65.5 Ma) (Fig. 10, top right); the effect of high O_2 with lower V_{cmax} is slightly reduced. The relatively low CO_2 during these periods also lowered A (Fig. 10, upper middle left). However, because the decrease is proportionally less than the decrease in C_a, C_i/C_a and $\Delta^{13}C$ both fall, producing an exaggerated near mirror image of the O_2 $\Delta^{13}C$ response (Fig. 10, upper middle right). This CO_2 response is damped rather than enhanced by the response of r to CO_2. It is not yet established whether r responds to O_2. The $\Delta^{13}C$ response to CO_2 at lower V_{cmax} is similar, shifted by ~0.6‰ for most of the Phanerozoic, except for the low CO_2 periods, when the shift is ⩽0.85‰, representing a small reduction in CO_2 sensitivity.

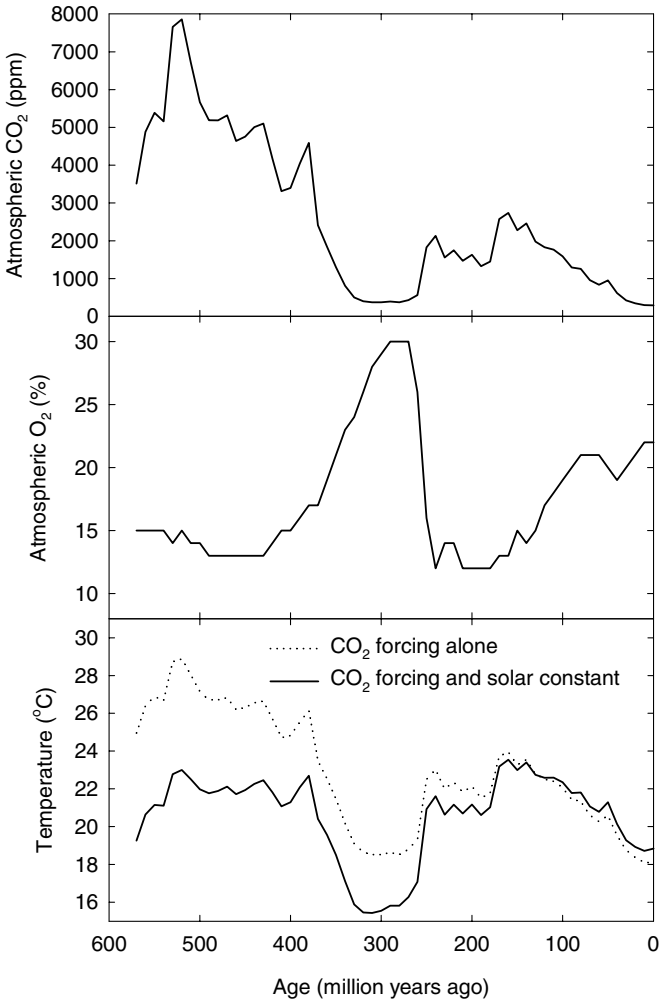

Fig. 9. Variation in (top) atmospheric CO_2, (middle) O_2, and (bottom) global mean temperature through the Phanerozoic. CO_2 data from Berner and Kothavala (2001), O_2 data from Berner (2001), and temperature after Beerling and Woodward (2001). Two temperature curves are shown, one based on the effects of CO_2, via the atmospheric greenhouse effect (dotted line), and the other on the effect of CO_2 and a 5% increase in the sun's output over the past 500 Myr (solid line).

As expected from earlier simulations, the effect of temperature is small in comparison with CO_2 and O_2, causing variation of <0.6‰ when the effect of increasing solar radiation on climate is taken into consideration (Fig. 10, lower middle panels). The effect at lower V_{cmax} is slightly greater, and in the opposite direction due to a shift in the balance of the effect of temperature on V_m and photorespiration. Although there is some inconsistency in the use of GEOCARB III CO_2 levels to estimate temperature, CO_2-independent methods such as the $\delta^{18}O$ record could be used; alternatively the model could be run iteratively until a

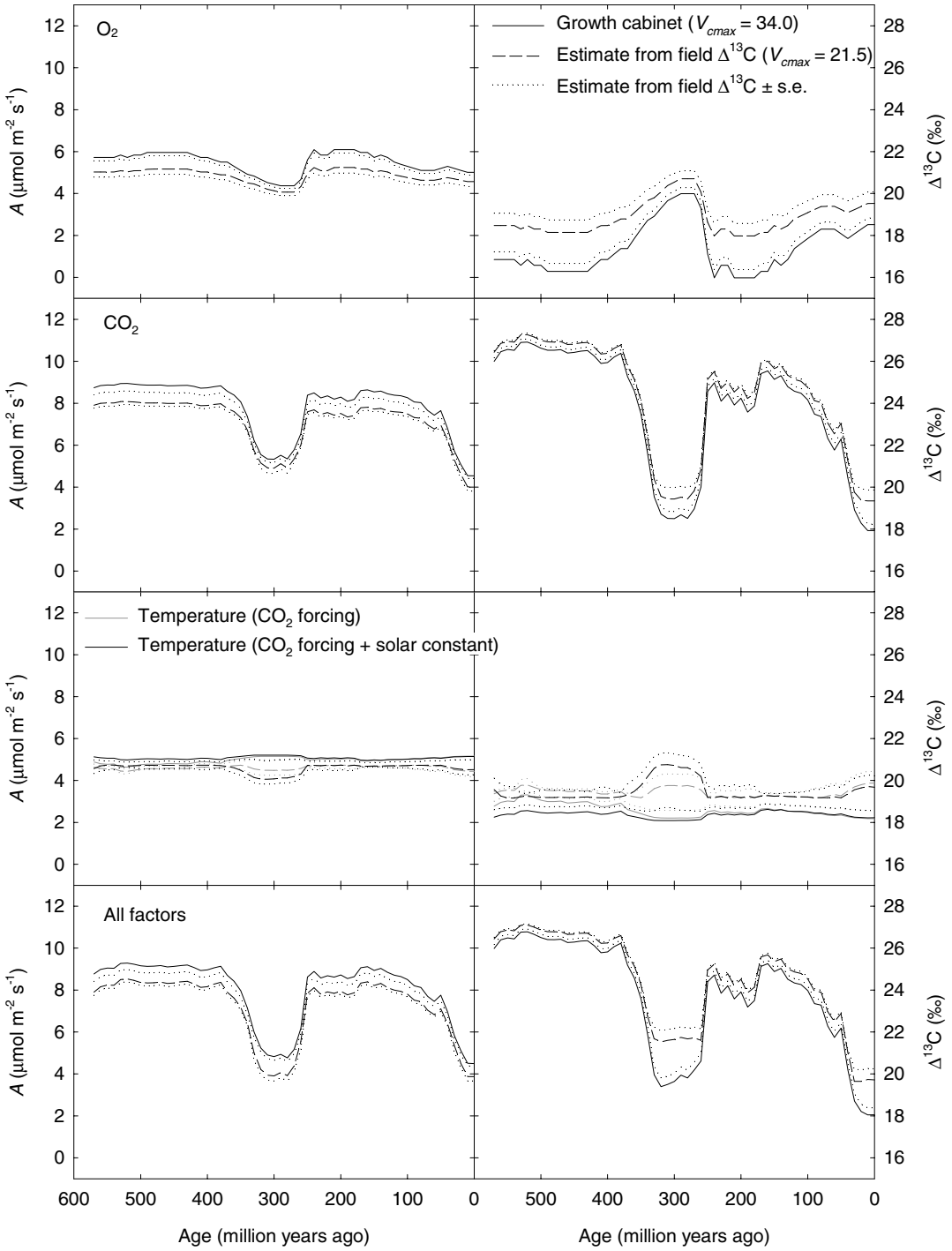

Fig. 10. Simulated separate and combined effects of variations in environmental conditions through the Phanerozoic on liverwort photosynthesis and $\Delta^{13}C$. The effect of O_2, CO_2 (r also responsive), and temperature CO_2 separately are shown in the top six panels, and that of all three factors combined in the lower two panels. Simulations are shown with temperature controlled (dotted line) by the effects of CO_2, via the atmospheric greenhouse effect, and (solid line) by both the effect of CO_2 and a 5% increase in the sun's output over the past 500 Myr. Standard conditions were 350 ppm CO_2, 21% O_2, 20 °C, 250 μmol PAR m^{-2} s^{-1}.

temperature-CO_2 consensus was reached. However, given the small effect of temperature on $\Delta^{13}C$, this is not likely to provide a significant source of error.

The simulated combined influence of CO_2, O_2 and temperature drive substantial variations in liverwort $\Delta^{13}C$ over the Phanerozoic, with values generally higher in those of modern populations (Fig. 10, bottom right panel). This result implies that the CO_2 signal in fossil bryophyte $\delta^{13}C$ could be discernable after accounting for other environmental conditions during the Phanerozoic. The extent of the increase in $\Delta^{13}C$ relative to the present-day varies with changes in atmospheric composition and

climate over time, being +5 to 7‰ in the Triassic, Jurassic and Cretaceous (251–65.5 Ma), ~+2‰ during the Permian and Late Carboniferous (318.1–251 Ma), and ~8‰ higher prior to the Middle Devonian (>397.5 Ma). At lower V_{cmax}, $\Delta^{13}C$ is higher during the low CO_2 periods and so these increases are ~1‰ reduced; for example, $\Delta^{13}C$ increases by ~5‰ between 1 and 100 Ma, instead of by ~6‰ with a V_{cmax} of 34. Estimates of $\Delta^{13}C$ from isotopic measurements on the fossil carbon of Cretaceous liverworts support these predictions, with values exceeding those of thallose liverworts in the Sheffield region by +5.1‰ (Fletcher et al., 2005). Clearly, however, the model is less sensitive to predicted CO_2 changes during the Silurian (443.7–416 Ma), where CO_2 is estimated to range between ~3000 and 5000 ppm CO_2 (~0.6‰), and in the Ordovician (488.3–443.7 Ma). However, the predictions of CO_2 at that time are highly uncertain, encompassing a very wide error range (Berner, 2004), and have to date only been compared with estimates from a single proxy (Yapp and Poths, 1992).

4.6. Comparative sensitivity of different stable carbon isotope-based CO_2 proxies

We compared the CO_2 sensitivity of liverwort $\Delta^{13}C$ with that of two leading CO_2 proxies based on $\delta^{13}C$ of fossil carbon of phytoplankton (Freeman and Hayes, 1992) and paleosols (Cerling, 1999), defined as ‰ ^{13}C discrimination per ppm CO_2, over the range of CO_2 experienced over the Phanerozoic. To facilitate comparisons between proxies, we expressed the change in $\delta^{13}C$ from 300 to 3000 ppm in $\Delta^{13}C$ (Fig. 11, left hand side). In each case, we varied one parameter to assess whether CO_2 sensitivity was affected. The variation between liverwort species' response of $\Delta^{13}C$ to CO_2 was simulated with a range of V_{cmax}, the primary variable determining differences in photosynthetic rate (Fig. 11, top panels). The liverwort $\Delta^{13}C$ sensitivity was compared with that for the phytoplankton species *Skeletonema costatum* grown at three temperatures (Hinga et al., 1994) (Fig. 11, middle panels). We converted $[CO_2]_{aq}$ to C_a using a linear fit based on the relationships

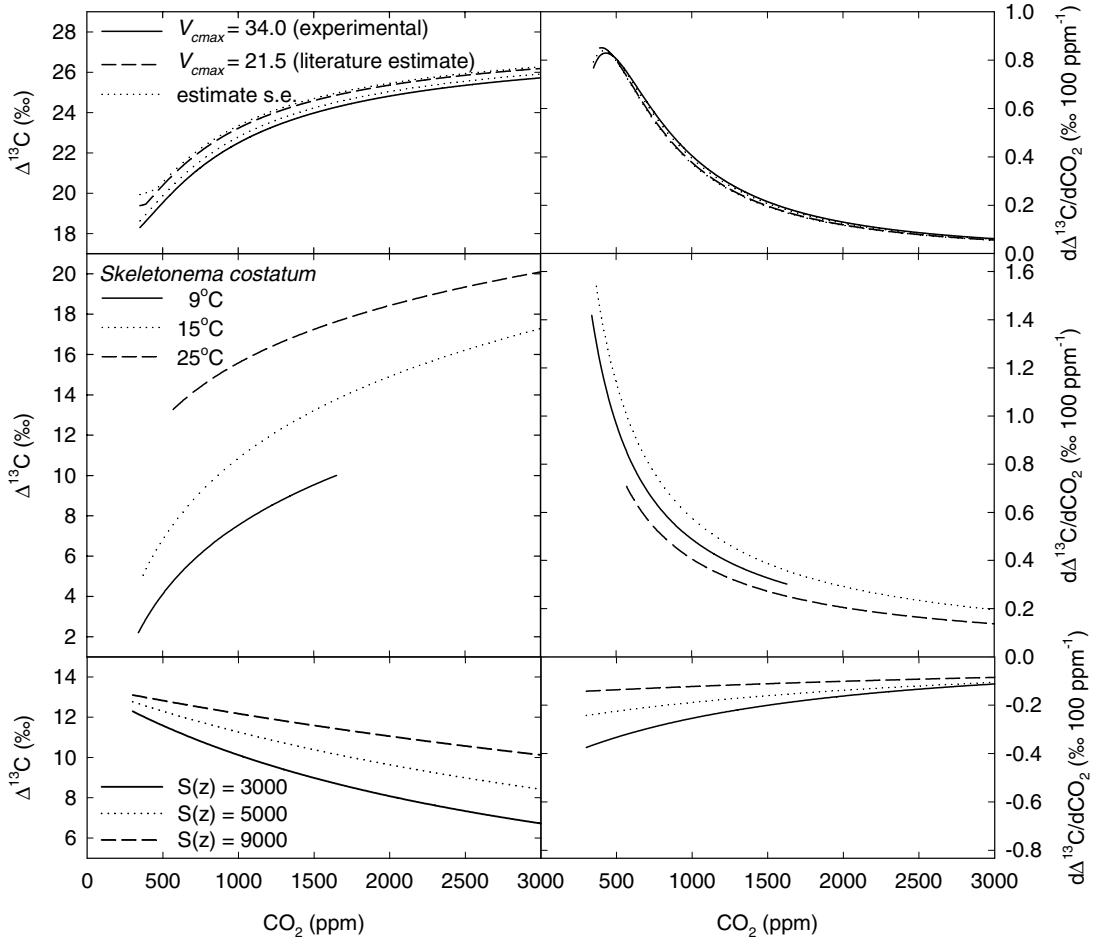

Fig. 11. A comparison of the sensitivity of proxy measures of CO_2 derived from the stable carbon isotope composition of liverworts (top), phytoplankton (middle), and paleosols (bottom), standardised as discrimination against ^{13}C (‰$\Delta^{13}C$), and as ‰$\Delta^{13}C$ 100 ppm^{-1}. A comparison of variables which can effect sensitivity is provided by varying the maximum rate of carboxylation in liverwort photosynthesis (from 34 μmol m^2 s^{-1} to 21.5 +6.5/−1.5 μmol m^2 s^{-1}); growth temperature in phytoplankton (from 9 to 15 °C), and the biologically respired soil CO_2 concentration in paleosols (from 3000 to 9000 ppm).

described in earlier studies (Freeman and Hayes, 1992), a conversion averaging out the effect of temperature and salinity. The comparison is intended to be illustrative for the phytoplankton rather than exhaustive. The response of paleosols was calculated from Cerling (1999) with three typical values for a major uncertainty $S(z)$, the concentration of CO_2 in the soil contributed by biological respiration (Cerling, 1999, see also Royer et al., 2001a).

The absolute response of these proxies over the range 300–3000 ppm CO_2 is in the order phytoplankton (12‰) > liverworts (7‰) > paleosols (5‰). However, as all of these proxies rely on proportional CO_2 changes, all are relatively more sensitive at low CO_2 (Fig. 11, right-hand side). Paleosols show the least the sensitivity, with a relatively constant response of 0.1–0.2‰ per 100 ppm change in CO_2, and phytoplankton the greatest, falling from ~1‰ per 100 ppm at around 500 ppm CO_2 to ~0.5‰ per 100 ppm at 1000 ppm and 0.25‰ per 100 ppm at 2000 ppm. The liverwort CO_2 proxy is intermediate between the two with rate of response declining from ~0.8‰ per 100 ppm at around 500 ppm CO_2 to ~0.4‰ per 100 ppm at 1000 ppm and 0.15‰ per 100 ppm at 2000 ppm; meaning that at high (>1000 ppm) CO_2, sensitivity is ~80% that of phytoplankton and ~2× that of paleosols. Although V_{cmax} may vary between laboratory growth experiments and field populations, affecting absolute CO_2 predictions, this change does not lessen the CO_2 sensitivity (Fig. 11, upper right panel) as, for example, increasing $S(z)$ does in paleosols (Fig. 11, lower right panel).

Clearly, estimates of parameters which affect CO_2 predictions such as temperature and O_2 have associated errors, and this is common to all proxies (reviewed by Royer et al., 2001a). Integrating all these possible sources of error and their probabilities into a measurement of error for a given CO_2 prediction may be achieved by using Bayesian methods to describe the proxy model followed by a Monte Carlo analysis. These methods include the errors associated with fitting parameters such as V_{cmax} and r, and produce a model which can be run thousands of times with all parameters allowed to vary, within a given range and probability, to produce a probability density function for CO_2 (Kennedy et al., in press). This type of Bayesian analysis is necessarily extensive in nature and will be addressed in a forthcoming paper.

5. Conclusion

Our aim was to develop a process-based model of liverwort isotope fractionation with the capacity to mechanistically account for the effects of CO_2, O_2, temperature and irradiance. The BRYOCARB model achieves this aim and is well validated against measurement of photosynthesis and $\Delta^{13}C$ under a range of conditions at different atmospheric CO_2 concentrations. BRYOCARB indicates that despite variations in environmental conditions and phenotypic plasticity in the photosynthetic physiology, CO_2 dominates isotopic discrimination in these bryophytes. Inversion of BRYOCARB (Appendix A) provides a mechanistic means of estimating of paleo-atmospheric CO_2 concentrations from fossil liverwort $\delta^{13}C$ measurements. Two key advantages of this proxy over its marine equivalent are first that it directly senses the atmospheric CO_2 concentration, and second that the signal can be reconstructed after mechanistically accounting for the effects of O_2 and temperature.

Acknowledgments

We thank Heather Walker for technical expertise that greatly eased our isotopic measurements and Peter Mitchell for helpful discussion concerning the light environment of woodlands. B.J.F. gratefully acknowledges funding from a University of Sheffield studentship. S.J.B. was funded through an NERC award to D.J.B. (NER/A/S/2001/00435). We are pleased to acknowledge Robert Berner's inspirational influence in our quest for biological approaches to assaying the composition of the ancient atmosphere.

Associate editor: David R. Cole

Appendix A. Determining CO_2 from liverwort $\Delta^{13}C$

An analytical solution of Eqs. (1)–(16) to determine the C_a given estimates of $\delta^{13}C_p$, $\delta^{13}C_a$, T, o_i; q, V_{cmax}, and r_d is not possible (see text for data sources). Here, $\delta^{13}C_p$ is taken as fossil liverwort $\delta^{13}C$ minus 1.85‰, to account for diagenesis (Fletcher et al., 2005). Therefore C_a is obtained by bisection. For a given value of $\Delta^{13}C$, the method involves calculating $\Delta^{13}C$ in the first instance from two seed values of C_a, 250 ppm ($C_{a\ low}$) and 25,000 ppm ($C_{a\ high}$).

The appropriate order of equation to obtain a solution is as follows: obtain r from Eq. (16), and τ, given by Eq. (A1):

$$\tau = \exp\left(-3.949 + \frac{28990}{RT}\right). \tag{A1}$$

Given $J_{max} = 1.64V_{cmax} + 29.1$ (Wullschleger, 1993), calculate V_m and J_m, and k_c and k_o (ppm) from the temperature dependent equations, as described earlier. The Rubisco-limited rate of photosynthesis (A_c) is then determined by first calculating C_i from Eqs. (12), (11) and (10), and the simplifying factor γ from Eq. (A2):

$$\gamma = 1 - \frac{o_i}{2\tau C_i}, \tag{A2}$$

and Eq. (5). The corresponding electron-transport limited rate of photosynthesis (A_j) is determined by first calculating C_i from Eqs. (15), (14) and (13), and J from Eq. (7), then Eq. (6). The minimum value A_c and A_j, together with its associated C_i is then used to determine $\delta^{13}C_p$ from Eq. (1), given the temperature sensitive CO_2 compensation point, Γ_* (ppm) (Brooks and Farquhar, 1985), and

fractionation due to molecular diffusion, a (4.4‰), photosynthesis effects, b (30‰), dark respiration, e (7‰), and photorespiration, f (2‰). Finally, Eq. (4) can be used to calculate $\Delta^{13}C$.

The next set of calculations are used to obtain values of C_a closer to that implied by the value of fossil liverwort $\Delta^{13}C$. Determine $\Delta^{13}C_{mean}$ as $\Delta^{13}C$ given C_a half way between the two initial values ($C_{a\ mean} = 0.5[C_{a\ low} + C_{a\ high}]$); if $\Delta_{13}C_{mean} >$ fossil $\Delta^{13}C$, let $C_{a\ high} = C_{a\ mean}$; if $\Delta^{13}C_{mean} <$ fossil $\Delta^{13}C$, let $C_{a\ low} = C_{a\ mean}$; repeat until $C_{a\_high} - C_{a\_low} <1$ ppm (at least $>\sim$16 times). This procedure assumes $\Delta^{13}C$ increases as C_a increases when $250 < C_a < 25{,}000$ which appears to hold true for most sensible combinations of parameters (known exceptions: very high q; very high r). The alternative is to calculate $\Delta^{13}C$ at $\leqslant$1ppm intervals for the given set of environmental conditions and physiological properties and 'read off' C_a from $\Delta^{13}C_{fossil}$. This process can be repeated for $\Delta^{13}C_{fossil} \pm 1$ s.e. where >1 specimen is analyzed to obtain the estimated within-population error.

References

Beerling, D.J., Royer, D.L., 2002. Fossil plants as indicators of the Phanerozoic global carbon cycle. *Ann. Rev. Earth Plan. Sci.* **153**, 387–397.

Beerling, D.J., Woodward, F.I., 2001. *Vegetation and The Terrestrial Carbon Cycle. Modelling the First 400 Million Years*. Cambridge University Press, Cambridge.

Beerling, D.J., Lake, J.A., Berner, R.A., Hickey, L.J., Taylor, D.W., Royer, D.L., 2002. Carbon isotope evidence implying high O_2/CO_2 ratios in the Permo-Carboniferous atmosphere. *Geochim. Cosmochim. Acta* **66**, 3757–3767.

Bergman, N.M., Lenton, T.M., Watson, A.J., 2004. COPSE: a new model of biogeochemical cycling over Phanerozoic time. *Am. J. Sci.* **304**, 397–437.

Berner, R.A., 1991. A model for atmospheric CO_2 over Phanerozoic time. *Am. J. Sci.* **291**, 339–376.

Berner, R.A., 2001. Modeling atmospheric O_2 over Phanerozoic time. *Geochim. Cosmochim. Acta* **65**, 685–694.

Berner, R.A., 1994. GEOCARB II: a revised model of atmospheric CO_2 over Phanerozoic time. *Am. J. Sci.* **294**, 56–91.

Berner, R.A., 2004. *The Phanerozoic carbon cycle: CO_2 and O_2*. Oxford University Press.

Berner, R.A., Kothavala, Z., 2001. Geocarb III: a revised model of atmospheric CO_2 over Phanerozoic time. *Am. J. Sci.* **301**, 182–204.

Berner, R.A., Petsch, S.T., Lake, J.A., Beerling, D.J., Popp, B.N., Lane, R.S., Laws, E.A., Westley, M.B., Cassar, N., Woodward, F.I., Quick, W.P., 2000. Isotope fractionation and atmospheric oxygen: implications for Phanerozoic O_2 evolution. *Science* **287**, 1630–1633.

Brooks, A., Farquhar, G.D., 1985. Effect of temperature on the CO_2-O_2 specificity of ribulose-1,5-biphosphate carboxylase/oxygenase and the rate of respiration in the light: estimates from gas exchange measurements on spinach. *Planta* **165**, 397–406.

von Caemmerer, S., Farquhar, G.D., 1981. Some relationships between the biochemistry of photosynthesis and the gas exchange of leaves. *Planta* **153**, 376–387.

Caldeira, K., Kasting, J.F., 1992. The life-span of the biosphere. *Nature* **360**, 721–723.

Cerling, T.E., 1991. Carbon dioxide in the atmosphere: evidence from Cenozoic and Mesozoic paleosols. *Am. J. Sci.* **291**, 377–400.

Cerling, T.E., 1999. Stable carbon isotopes in paleosol carbonates. *Spec. Publ. Int. Ass. Sediment.* **27**, 43–60.

Farquahar, G.D., von Caemmerer, S., Berry, J.A., 1980. A biochemical model of photosynthetic CO_2 assimilation in leaves of C_3 species. *Planta* **149**, 78–90.

Farquhar, G.D., O'Leary, M.H., Berry, J.A., 1982. On the relationship between carbon isotope discrimination and the intercellular carbon dioxide concentration in leaves. *Aust. J. Plant Physiol.* **9**, 121–137.

Farquhar, G.D., Ehleringer, J.R., Hubick, K.T., 1989. Carbon isotope discrimination and photosynthesis. *Ann. Rev. Plant Phys. Plant Mol. Biol.* **40**, 503–537.

Field, C., Mooney, H.A., 1986. The photosynthesis-nitrogen relationship in wild plants. In: Givnish, T.J. (Ed.), *On the Economy of Plant Form and Function*. Cambridge University Press, Cambridge, pp. 25–55.

Figge, R.A., White, J.W.C., 1995. High-resolution Holocene and late glacial atmospheric CO_2 record: variability tied to changes in thermohaline circulation. *Global Biogeochem. Cycles* **9**, 391–403.

Fletcher, B.J., Beerling, D.J., Chaloner, W.G., 2004. Stable carbon isotopes and the metabolism of the terrestrial Devonian organism Spongiophyton. *Geobiology* **2**, 107–119.

Fletcher, B.J., Beerling, D.J., Brentnall, S.J., Royer, D.L., 2005. Fossil bryophytes as recorders of ancient CO_2 levels: experimental evidence and a Cretaceous case study. *Global Biogeochem. Cycles* **19**, GB3012, doi:10.1029/2005GB002495.

Freeman, K.H., Hayes, J.M., 1992. Fractionation of carbon isotopes by phytoplankton and estimates of ancient CO_2 levels. *Global Biogeochem. Cycles* **6**, 185–198.

Gillon, J.S., Griffiths, H., 1997. The influence of (photo)respiration on carbon isotope discrimination in plants. *Plant Cell Environ.* **20**, 1217–1230.

Gimeno, C., Deltoro, V.I., 2000. Sulphur dioxide effects on cell structure and photosynthetic performance in the liverwort *Frullania dilatata*. *Can. J. Bot.* **78**, 98–104.

Green, T.G.A., Lange, O.L., 1995. Photosynthesis in poikilohydric plants: a comparison of lichens and bryophytes. In: Schulze, E.D., Caldwell, M.M. (Eds.), *Ecophysiology of Photosynthesis*. Springer-Verlag, New York, pp. 319–341.

Green, T.G.A., Snelgar, W.P., 1983. A comparison of photosynthesis in two thalloid liverworts. *Oecologia* **54**, 275–280.

Griffiths, H., Maxwell, K., Richardson, D., Robe, W., 2004. Turning the land green: inferring photosynthetic physiology and diffusive limitations in early bryophytes. In: Hemsley, A.R., Poole, I. (Eds.), *The Evolution of Plant Physiology from Whole Plants to Ecosystem*. Elsevier, New York, pp. 3–16.

Hamerlynck, E.P., Csintalan, Z., Nagy, Z., Tuba, Z., Henebry, G.M., 2002. Ecophysiological consequences of contrasting microenvironments on the desiccation tolerant moss, *Tortula ruralis*. *Oecologia* **131**, 498–505.

Harley, P.C., Thomas, R.B., Reynolds, J.F., Strain, B.R., 1992. Modelling photosynthesis of cotton grown in elevated CO_2. *Plant Cell Environ.* **15**, 271–282.

Hinga, K.R., Arthur, M.A., Pilson, M.E.Q., Whitaker, D., 1994. Carbon isotope fractionation by marine plankton in culture: the effect of CO_2 concentration, pH, temperature, and species. *Global Biogeochem. Cycles* **8**, 91–102.

Kashiwagi, H., Shikazono, N., 2003. Climate change during Cenozoic inferred from global carbon cycle model including igneous and hydrothermal activities. *Palaeogeogr. Palaeoclimatol. Palaeoecol.* **199**, 167–185.

Kennedy, M.C., Anderson, C.W., Conti, S., O'Hagan, in press. Case studies in Gaussian process modelling of computer codes. *Reliability Engineering & System Safety*.

Kübler, J.E., Johnston, A.M., Raven, J.A., 1999. The effects of reduced and elevated CO_2 and O_2 on the seaweed *Lomentaria articulata*. *Plant Cell Environ.* **22**, 1303–1310.

Lawlor, D.W., 1993. *Photosynthesis. Molecular, Physiological and Environmental Processes*, second ed. Longman Scientific and Technical, Essex.

Laws, E.A., Popp, B.N., Bidigare, R.R., Kennicutt, M.C., Macko, S.A., 1995. Dependence of phytoplankton carbon isotopic composition on growth rate and $[CO_2]_{aq}$: theoretical considerations and experimental results. *Geochim. Cosmochim. Acta* **59**, 1131–1138.

Laws, E.A., Popp, B.N., Cassar, N., Tanimoto, J., 2002. ^{13}C discrimination patterns in oceanic phytoplankton: likely influence of CO_2 concentrating mechanisms, and implications for palaeoreconstructions. *Funct. Plant Biol.* **29**, 323–333.

Long, S.P., 1991. Modification of the response of photosynthetic productivity to rising temperature by atmospheric CO_2 concentrations: has its importance been underestimated? *Plant Cell Environ.* **14**, 729–739.

Long, S.P., Ainsworth, E.A., Rogers, A., Ort, D.R., 2004. Rising atmospheric carbon dioxide: plants FACE the future. *Annu. Rev. Plant Biol.* **55**, 591–628.

Marschall, M., Proctor, M.C.F., 2004. Are bryophytes shade plants? Photosynthetic light responses and proportions of chlorophyll *a*, chlorophyll *b* and total carotenoids. *Ann. Bot.* **94**, 593–603.

McElwain, J.C., Chaloner, W.G., 1995. Stomatal density and index of fossil plants track atmospheric carbon dioxide in the Palaeozoic. *Ann. Bot.* **76**, 389–395.

Mitchell, P.L., 1992. Growth stages and microclimate in coppice and high forest. In: Buckley, G.P. (Ed.), *Ecology and Management of Coppice Woodlands*. Chapman & Hall, London, pp. 35–51.

Pagani, M., Arthur, M.A., Freeman, K.H., 1999. Miocene evolution of atmospheric carbon dioxide. *Paleoceanography* **14**, 273–292.

Pearson, P.N., Palmer, M.R., 2000. Atmospheric carbon dioxide concentrations over the past 60 million years. *Nature* **406**, 695–699.

Popp, B.N., Laws, E.A., Bidigare, R.R., Dore, J.E., Hanson, K.L., Wakeham, S.G., 1998. Effect of phytoplankton cell geometry on carbon isotope fractionation. *Geochim. Cosmochim. Acta* **62**, 69–77.

Proctor, M.C.F., 1982. Physiological ecology: water relations, light and temperature responses, carbon balance. In: Smith, A.J.E. (Ed.), *Bryophyte Ecology*. Chapman and Hall, London, pp. 333–381.

Royer, D.L., Berner, R.A., Beerling, D.J., 2001a. Phanerozoic atmospheric CO_2 change: evaluating geochemical and paleobiological approaches. *Earth Sci. Rev.* **54**, 349–392.

Royer, D.L., Wing, S.L., Beerling, D.J., Jolley, D.W., Koch, P.L., Hickey, L.J., Berner, R.A., 2001b. Paleobotanical evidence for near present-day levels of atmospheric CO_2 during part of the Tertiary. *Science* **292**, 2310–2313.

Swanson, R.V., Flanagan, L.B., 2001. Environmental regulation of carbon dioxide exchange at the forest floor in a boreal black spruce ecosystem. *Agric. Forest Meteorol.* **108**, 165–181.

Tajika, E., 1998. Climate change during the last 150 million years: reconstruction from a carbon cycle model. *Earth Planet. Sci. Lett.* **160**, 695–707.

Van der Burgh, J., Visscher, H., Dilcher, D.L., Kürschner, W.M., 1993. Paleoatmospheric signatures in Neogene fossil leaves. *Science* **260**, 1788–1790.

Wallmann, K., 2001. Controls on the Cretaceous and Cenozoic evolution of seawater composition, atmospheric CO_2 and climate. *Geochim. Cosmochim. Acta* **65**, 3005–3025.

White, J.W.C., Ciais, P., Figge, R.A., Kenny, R., Markgraf, V., 1994. A high-resolution record of atmospheric CO_2 content from carbon isotopes in peat. *Nature* **367**, 153–156.

Williams, T.G., Flanagan, L.B., 1998. Measuring and modelling environmental influence on photosynthetic gas exchange in *Sphagnum* and *Pleurozium*. *Plant Cell Environ.* **108**, 38–46.

Wullschleger, S.D., 1993. Biochemical limitations to carbon assimilation in C_3 plants—a retrospective analysis of the curves from 109 species. *J. Exp. Bot.* **44**, 907–920.

Yapp, C.J., Poths, H., 1992. Ancient atmospheric CO_2 pressures inferred from natural goethites. *Nature* **137**, 71–82.